

Three Dimensional Volume Reconstruction of an Object from X-ray Images

Y.J. Roh^a, B.M. Kim^a, H.S. Cho^a, H.C Kim^b

^aDept. of Mechanical Eng., Korea Advanced Institute of Science and Technology

^bFA Research Institute Production Engineering Center, Samsung Electronics Co., LTD

ABSTRACT

Inspection and shape measurement of three-dimensional objects are widely needed in industries for quality monitoring and control. A number of visual or optical technologies have been successfully applied to measure three dimensional surfaces. However, those conventional visual or optical methods have inherent shortcomings, which are occlusion problem and variant surface reflection problem. X-ray vision system can be a good solution to these conventional problems, since we can extract the volume information including both the surface geometry and the inner structure of the object. In the x-ray system, the surface condition of an object, whether it is lambertian or specular, does not affect the inherent characteristics of its x-ray images. In this paper, we propose a three dimensional x-ray imaging method to reconstruct a three dimensional structure of an object out of two dimensional x-ray image sets. To achieve this by this method, more than two x-ray images projected from different views are needed. Once these images are acquired, the simultaneous algebraic reconstruction technique(SART) is usually utilized at present. Since the existing SART algorithms have several shortcomings such as low performance in convergence and different convergence within the reconstruction volume of interest, an advanced SART algorithm named as USART(uniform SART) is proposed here to avoid the shortcomings and improve the reconstruction performance. In this method, each voxel within the volume is equally weighted to update instantaneous value of its internal density, thereby achieving uniform convergence property of the reconstructed volume. The algorithm is simulated on various shapes of objects such as a pyramid, a hemisphere and a BGA model, then the performance of the proposed method is compared with that of the conventional SART method.

Keywords : x-ray, 3D reconstruction, algebraic reconstruction technique, inspection.

1. INTRODUCTION

Three dimensional shape measurement techniques are widely needed in industries for product quality monitoring and control. A number of visual or optical methods have been developed for that purpose using laser structured light, moire, stereo vision, confocal microscope and so on. However, those conventional visual or optical methods have inherent shortcomings, which are occlusion problem and variant surface reflection problem. Thus the applications are restricted to the special objects as measuring methods¹⁻².

On the other hand, x-ray vision method can be a good solution to overcome these conventional problems, since we can extract the volume information including both the surface geometry and the inner structure of the object. In x-ray system, the surface condition of an object, whether it is lambertian or specular, does not affect the inherent characteristics of its x-ray images. By those advantages, it is frequently used in industries for the quality inspection of electronic goods such as memory chips, camcorders or cellular phones. In certain applications, three dimensional x-ray imaging techniques are needed for the precise measurements or inspections. Ball grid array(BGA) and chip-scale package(CSP) which are widely used in high-density PCB can be good applications of that. In that cases, the lead bumps and solder joints are located underneath its own

Correspondence : Email : hscho@lca.kaist.ac.kr ; WWW : <http://lca.kaist.ac.kr> ; Telephone : +82-42-869-3253

package as shown in Figure 1. To inspect quality of them precisely, whether the solder joints are well attached with adequate soldering quantities or there are void defects within them, the inspection methods based on three dimensional images of them are needed³⁻⁷.

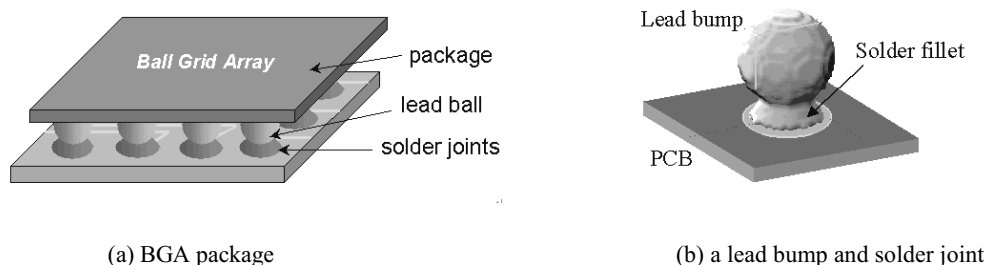


Figure 1. BGA package and its joint parts

There are several techniques to acquire a three dimensional information using x-ray images. The most traditional and the simplest way is to take a series of the cross-sectional images layer by layer and build a three dimensional image with them. The cross-sectional images can be made by computed tomography, laminography or digital tomosynthesis(DT) techniques. However, computed tomography requires a hard conditions that each cross-section of the object needs to be projected from all directions and it can not be possible in many applications⁸. The cross-sectional images made by laminography or DT include inherent errors by artifacts or blurring effects, thus the 3D volume built by them will be a different one⁹⁻¹⁰.

Rather than that, another method can be utilized to reconstruct a three dimensional structure of an object directly out of two dimensional x-ray image sets. To achieve this, more than two x-ray images projected from different projection views are needed. By using these images, algebraic reconstruction technique(ART), an iterative computation method, is used to estimate their three dimensional volume. Here, the three dimensional object is represented by finite number of volume elements, voxels with their own density values. Then, the density values of the voxels are determined from the information of their projections by the reconstruction algorithms¹¹⁻¹⁵. Though the reconstruction accuracy is mainly depend on the imaging conditions, there is no hard restriction to the imaging conditions for this method. Simultaneous ART is one of the advanced forms of the basic ART, and it accomplished a better convergence and reduced the salt-noise in the reconstructed volume. However, the SART algorithm also has some shortcomings such as low efficiency in its computation and different convergence within the reconstruction volume of interest¹⁶.

In this paper, the advanced ART algorithm named as USART(uniform and simultaneous ART) is proposed to avoid those shortcomings and improve the reconstruction performance. In this method, each voxels within the volume is equally weighted to update instantaneous value of its internal density, thereby achieving uniform convergence property of the reconstructed volume. The algorithm is simulated on various shapes of objects such as cone, hemisphere and BGA model. Also the performance of the proposed method is compared with that of the conventional SART method.

2. X-ray image acquisition

2.1 X-ray images from different views

To reconstruct the three dimensional structure of an object, two or more x-ray images which are projected from different directions are needed. The imaging conditions such as the number of images and their view points for acquiring sufficient information of the object are problem dependent. There are several choices to take a different view of the object. One is rotating the object for arbitrary axis within the x-ray imaging area, but it is some difficult to realize it practically and its application is restricted to the special objects to be handled as that way.

Instead moving the x-ray source and the image plane relatively to the object will be a more general imaging method. In general the x-ray can be understood as a point light source and an x-ray image is a shadow of an object on a image plane by a cone beam geometry. Thus, the geometric imaging conditions depend on the relative coordinates of the x-ray source and the imaging plane with respect to the object. Figure 2 shows a general cone beam x-ray imaging geometry. As the relative positions of the x-ray source and the image plane to the object are varied, which is represented by the superscript index 1 to 2 in this figure, the images projected from different views can be acquired.

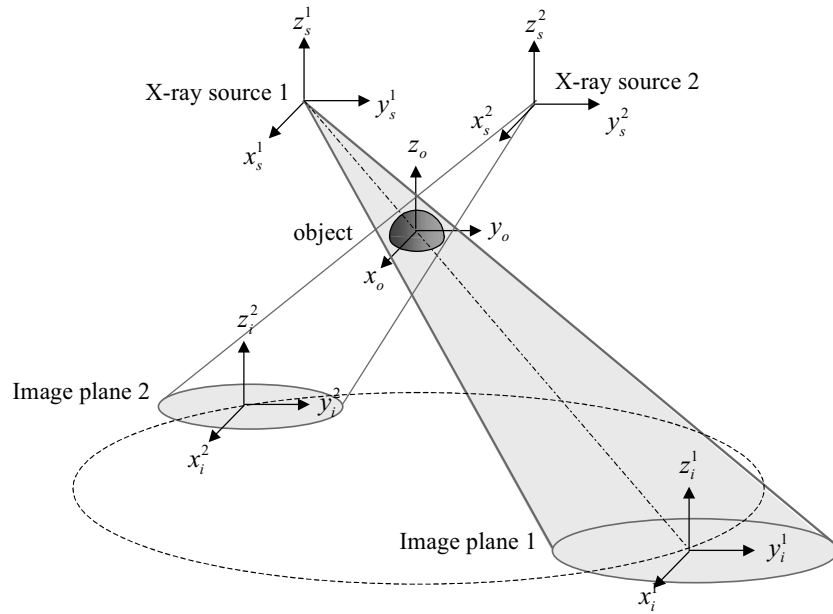


Figure 2. X-ray imaging geometry

2.2 X-ray system configuration

Figure 3 shows the structure of the developed x-ray system, which consists of a scanning x-ray tube, an image intensifier, a rotating prism and a camera equipped with a zoom lens. The scanning x-ray tube is designed to electrically control the position of an x-ray spot, and to project an x-ray beam into an object from different directions. Attenuated x-rays passing through the object are collected by an image intensifier, and converted into a visible image on the instrument's output screen.

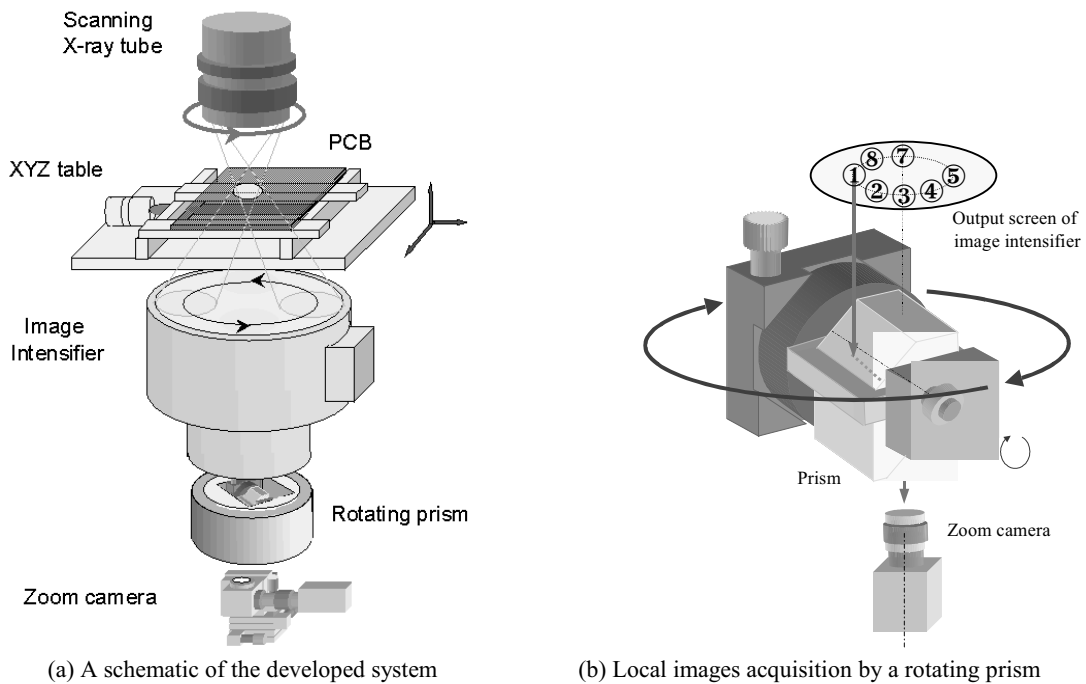


Figure 3. The structure of the developed 3D x-ray imaging system

The object is projected on a circular trajectory on the image intensifier as the x-ray is steered, and eight or more images are sequentially acquired by the zoom camera through the rotating prism. The prism rotates in synchronization with the x-ray position to capture the projected images on the screen of image intensifier as shown in figure 3 (b). The images captured at different positions are saved in the digital memory of a computer, and then processed to generate a three dimensional image of the object. Practically, image correction processes are needed, since the curved input surface of the image intensifier distorts the images¹⁷⁻¹⁸.

3. 3D volume reconstruction using UART algorithm

The 3D area to be reconstructed here is represented by finite number of volume elements, voxels. Then an arbitrary 3D object made with various materials can be represented by the voxels with their own densities respectively. The resolution of the object by this representation method is depend on the number of voxels. And it is the 3D reconstruction problem that the density values for the voxels are determined from the projected 2D x-ray images. The simultaneous algebraic reconstruction technique(SART) is a method to solve the problem. However, the existing SART algorithms have several shortcomings such as low performance in convergence and different convergence within the volume to be reconstructed, the advanced SART algorithm named as USART(uniform SART) is proposed here to avoid the shortcomings and improve the reconstruction performance.

3.1 Modeling of the forward projection process

At first, the image projection process (e.g. a 3D volume into a 2D image plane or a 2D image into a 1D array) needs to be modeled considering the object representing method. As noted previously, the object is described by a finite number of discrete elements, pixels or voxels. We assume that the projection image depends linearly on the density of the object and also the length of intersection of a ray within the object. It is modified later as a non-linear model of the x-ray imaging process, which is a more close to the practical one. Then, the x-ray projection process is modeled as the equation (1), which represents the linear combination of the density values and the intersection length of the elements, pixels or voxels, by a ray¹¹⁻¹⁴.

$$y^j(t) = \sum_{i=1}^N a_i^j \cdot x_i(t) \tag{1}$$

In this equation y^j is a projection value of the j^{th} ray, x_i is the density value of the i^{th} element, and a_i^j is the intersection length of the i^{th} element by the j^{th} ray. The meaning of the equation (1) is illustrated as in the figure 4 for a simplified 2D case.

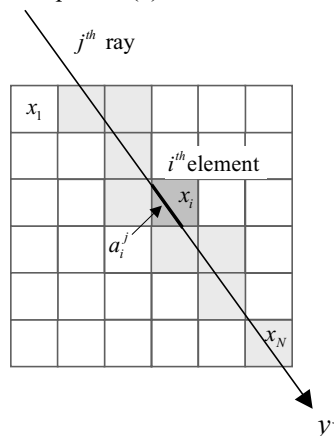


Figure 4. A model of the transmission image.

Then, our task is to determine the unknown density values of x_i based on the measured values of the transmission g^j . And one can assume in this problem that the intersection lengths a_i^j can be calculated from the known geometry of the imaging conditions. Equation (1) can be rewritten as a matrix form of equation (2), which includes M linear equations with N

unknown values of x_i .

$$\mathbf{y} = \mathbf{A}\mathbf{x} \quad (2)$$

$$\mathbf{A} = \begin{bmatrix} a_1^1 & a_2^1 & \cdots & a_N^1 \\ a_1^2 & a_2^2 & \cdots & a_N^2 \\ \vdots & \vdots & \vdots & \vdots \\ a_1^M & a_2^M & \cdots & a_N^M \end{bmatrix} = \begin{bmatrix} \mathbf{a}^1 \\ \mathbf{a}^2 \\ \vdots \\ \mathbf{a}^M \end{bmatrix}$$

$$\mathbf{x} \in R^N, \mathbf{y} \in R^M, \mathbf{A} \in R^{M \times N}$$

3.2 Basic ART and SART algorithm

The reconstruction process is to solve the equation (2) and estimate the density values of the object \mathbf{x} . The equation looks simple and easy to be solved. But in practice the size of the matrixes in the equation are too huge to be solved by a direct method (e.g. a method based on the singular value decomposition of \mathbf{A} or a pseudo-inverse of \mathbf{A}). Instead, iterative schemes are used which avoid the waste of memory and computation time in computer. One of them is a well known algebraic reconstruction technique(ART) algorithm and a series of its modified versions are available. Using the notation used above, the solution of the equation (1) can be acquired by recursive computations denoted by the equation (3).

$$x_i(t+1) = x_i(t) + \lambda \frac{g^j - y^j(t)}{\sum_i (a_i^j)^2} a_i^j \quad (3)$$

The equation (3) presents an update scheme for an i^{th} element x_i based on a measurement of the j^{th} ray g^j and its estimation y^j . In this equation, t is the iteration time step and λ is an update constant which has the values between 0.8 and 1.2. Considering lots of equations for all the rays, the equation (3) can be written as a matrix form, which is more compact and easy to be understood.

$$\mathbf{x}(t+1) = \mathbf{x}(t) + \lambda \frac{g^j - y^j(t)}{\|\mathbf{a}^j\|^2} \mathbf{a}^j \quad (4)$$

$$j=1,2,\dots,M$$

From the above equation, the estimate vector of the object $\mathbf{x} = \{x_i | i=1,2,\dots,N\}$ is updated when a measurement for each ray is considered. Thus, one epoch of the update is completed when all M rays are used for the modification of the estimates.

It has been known that a modified version of ART of which the name is the simultaneous ART(SART) gives better results than the basic ART. In the SART, the error correction terms for all rays are considered simultaneously and the estimates of the object x_i are updated at a time rather than in the sequential fashion. SART is expressed as the equation (5), where all error terms for the rays $g^j - \mathbf{a}^j \mathbf{x}(t)$ $j=1,2,\dots,M$ are included in that¹⁴.

For i^{th} element x_i ,

$$x_i(t+1) = x_i(t) + \lambda \frac{\sum_{j=1}^M a_i^j \frac{g^j - y^j(t)}{\sum_{i=1}^N a_i^j}}{\left\| \sum_{j=1}^M \mathbf{a}^j \right\|} \quad (5)$$

As the number of iterations of the algorithm increases, the error terms gradually go to smaller values thus the estimate vector of the object \mathbf{x} converges to the real one. The convergence will ultimately depend on the accuracy of the discrete representation of the forward projection process and the accuracy of the measurements.

3.3 Uniform SART algorithm

In the conventional SART algorithm, the ray geometry vectors $\mathbf{a}^j, j = 1, 2, \dots, M$ are calculated in advance based on the imaging conditions. X-ray is a point light source and modeled as a fan beam or a cone beam in 2D or 3D problems respectively. There are uncountable rays passing through the object, but only a finite number of measurements are available in practice according to the resolution of the sensing unit. And the rays considered in the computations depend on it. The more rays are considered in the update algorithm, the better estimate result should be guaranteed. However, the resolutions of the measurements are limited practically and considering a large number of rays need also huge memory size and computation time as well. Thus if we formulate the ray geometry vectors for the rays traced from a x-ray source to the x-ray image elements, the rays pass through the object un-uniformly within the reconstruction area. Especially, the effect will be dominant in case of the limited view of projection. The situation is illustrated in figure 5, in which the larger number of rays pass the elements in the upper or close to the x-ray side of the reconstruction area. It may result in different convergence within the reconstruction area, and it can not be solved by just enlarging the image resolution and the number of rays¹⁶.

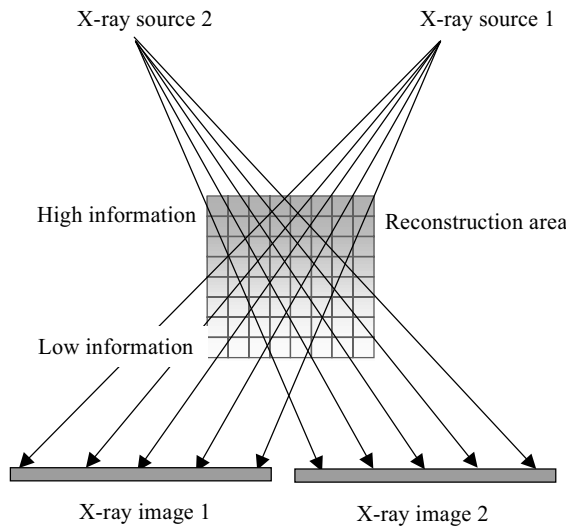


Figure 5. Un-uniformly passing rays within the object

Rather than that, more efficient rules for selecting or generating the rays for the updates are needed in the implementation. Our interest here is focused on an element that is to be updated and then only the rays that passes through the center of each element are considered. Thus, there are V rays across the center of the i^{th} element if the number of views for the projections is V .

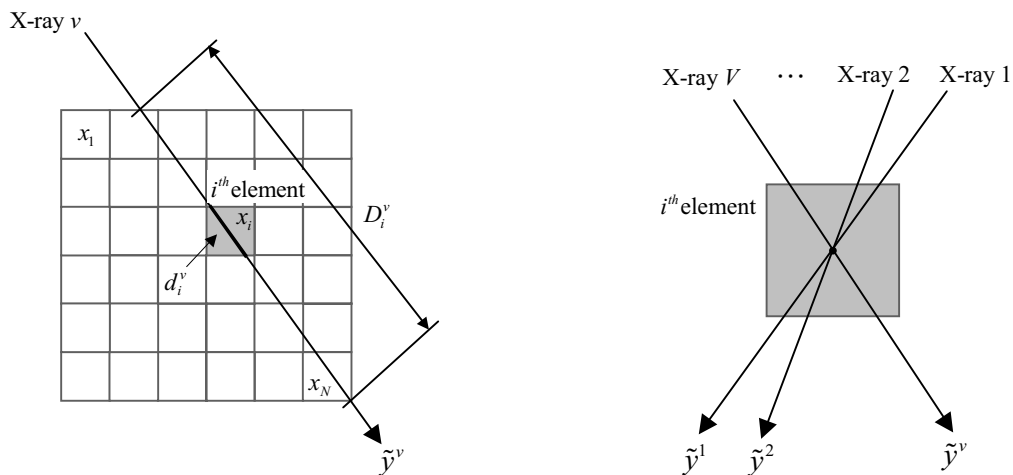


Figure 6. Rays pass through the element in USART

In this situation, the ray ν transmits the i^{th} element and the whole reconstruction area with the length of d_i^ν and the D_i^ν respectively. And S_i is the summation of the d_i^ν s of the all views for the i^{th} element. Then the density value of the i^{th} element $x_i(t)$ is updated by the equation (6). It is noticeable that the measurements g^ν and the projection of the estimated object y^ν for the ray ν can not be acquired directly, since the ray ν is just a temporarily considered ray for convenience. Thus the values are replaced to \tilde{g}^ν and \tilde{y}^ν , the interpolation values of the g^ν and y^ν respectively.

$$x_i(t+1) = x_i(t) + \lambda \frac{\sum_{\nu=1}^V \frac{d_i^\nu}{D_i^\nu} (\tilde{g}^\nu - \tilde{y}^\nu)}{S_i} \quad (6)$$

$$S_i = \sum_{\nu=1}^V d_i^\nu, \quad i=1,2,\dots,N$$

3.4 USART algorithm using x-ray imaging model

In the above, the projection process was simplified as a linear combinations of the transmittance length and a density values of the object for convenience. However, the projections by the x-ray need an exponential model additionally, and the linear model (1) is modified as the equation (7).

$$y^j = y_0 \exp\left(-\sum_{i=1}^N a_i^j x_i\right) \quad (7)$$

It can be thought that x_i is the absorption coefficient of the i^{th} object element and a_i^j is the pass-through length of the j^{th} ray within the element. And in that case, the USART algorithm of the equation (6) is simply modified to the equation (8).

$$x_i(t+1) = x_i(t) + \lambda \frac{\sum_{\nu=1}^V \frac{d_i^\nu}{D_i^\nu} \ln \frac{\tilde{g}^\nu}{\tilde{y}^\nu}}{S_i} \quad (8)$$

$$i=1,2,\dots,N$$

4. Simulations

4.1 Experimental conditions

We tested the proposed USART algorithm as a simulation study to the reconstruction problems of the basic objects such as a pyramid, a hemisphere and also a model of BGA joint. All the parameters used in the simulations are selected considering practical imaging conditions of the 3D x-ray system built in. The main parameters or factors used in the simulation are listed in Table 1.

Table 1. X-ray DT imaging conditions

Main parameters	Conditions
X-ray view angle w.r.t the center axis	30 (degree)
Number of the views	8
Image resolution	80 x 80 (pixel)
Reconstructed volume area	1 x 1 x 1 (mm)
Number of voxels	40 x 40 x 40 voxel

The application is focused here on the 3D reconstruction of the BGA joint, of which size is within $1 \times 1 \times 1 \text{mm}$ volume. The object models used in the simulation are shown in the figure 7.

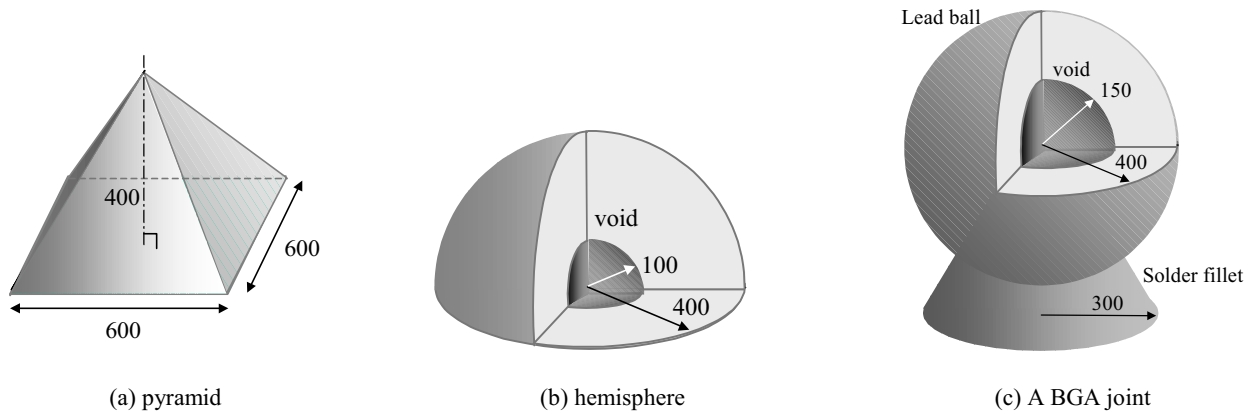


Figure 7. Objects used in the simulations (unit : micrometer)

4.2 Evaluation of the reconstruction error

The performance of the ART algorithm can be evaluated based on errors of the reconstructed volume. And it is defined as an error between the reference volume and its reconstructed one. Since a three dimensional object is represented by a finite number of volume elements in this research, the volume error can be evaluated by a direct comparison of the corresponding elements between the two volumes. As a form of root mean square(RMS) error, it is defined as the equation (9). In the definition, o_i and x_i are density values of the i^{th} element in a reference volume and in a reconstructed volume respectively.

$$E_{volume} = \sqrt{\frac{1}{N} \sum_{i=1}^N \frac{(o_i - x_i)^2}{o_i^2}} \times 100 \quad (\%) \quad (9)$$

The above volume error can be evaluated only to the known object, and it is just a measure of the performance of the reconstruction algorithm. From the view-point of the evaluation of the iterations, whether these process is being converged to a desired volume, another definition of the process error needs to be considered. In the recursive processes, the error terms which drive the estimated volume $\mathbf{x}(t)$ to a modified one $\mathbf{x}(t+1)$ are $g^j - y^j(t)$ and $\tilde{g}^j - \tilde{y}^j(t)$ terms in the equation (5) and (6) respectively. Their physical meanings are the errors of a projection $\mathbf{y}(t)$ of the estimated volume $\mathbf{x}(t)$ to the measured projection \mathbf{g} at an iteration step t . By using these error terms, the projection image error is defined as the equation (10) and it represents the averaged intensity error of the estimated image. There is no update to the volume if there is no meaningful projection image error in the reconstruction process.

$$E_{img} = \sqrt{\frac{1}{V \times R} \|\mathbf{g} - \mathbf{y}(t)\|^2} \quad (10)$$

R : number of pixels of a projection image

V : number of views

4.3 Simulation results

Figure 8 illustrates the processes of the volume reconstruction by using USART algorithm for a BGA joint model. As the iterations proceed, the volume was updated and converged to the close to the reference one. After 60 iterations, there was no remarkable change in the volume. The initialized volume for the recursive calculations was made by the digital tomosynthesis technique which can generate a series of cross-sections roughly from the given x-ray images^{16, 18-20}.

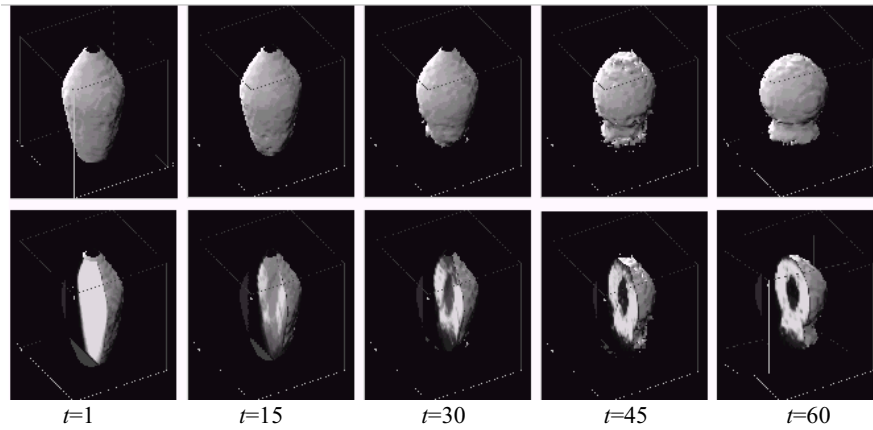
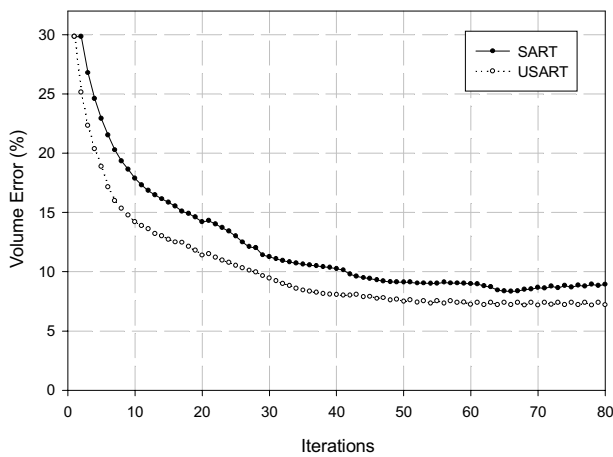
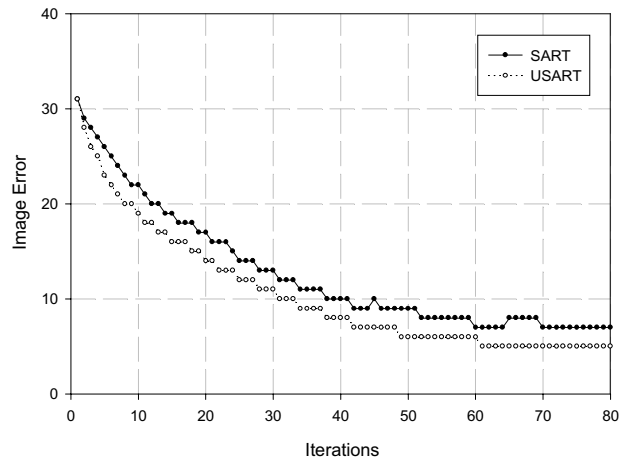


Figure 8. The reconstruction results for the iterations

Figure 9 shows the error convergence in the reconstruction of the BGA joint by SART and USART methods. Figure 9. (a) and (b) represent the convergence of the volume error and that of the image error respectively. From the error plots, we can argue that the USART method is superior to the conventional SART method in that the errors of the USART was converged faster and also their final values were smaller than those of SART.



(a) Volume error convergence



(b) Image error convergence

Figure 9. Comparison of the error convergence between SART and USART

Figure 10 shows the reconstructed three dimensional volumes for the objects, pyramid, hemisphere and a BGA joint, used in the simulations. The results show that the surface shapes and also their inner structures were well reconstructed and their volume errors were 5 ~ 7 %. And the image errors converged to 5 gray value in case of 8 bit images.

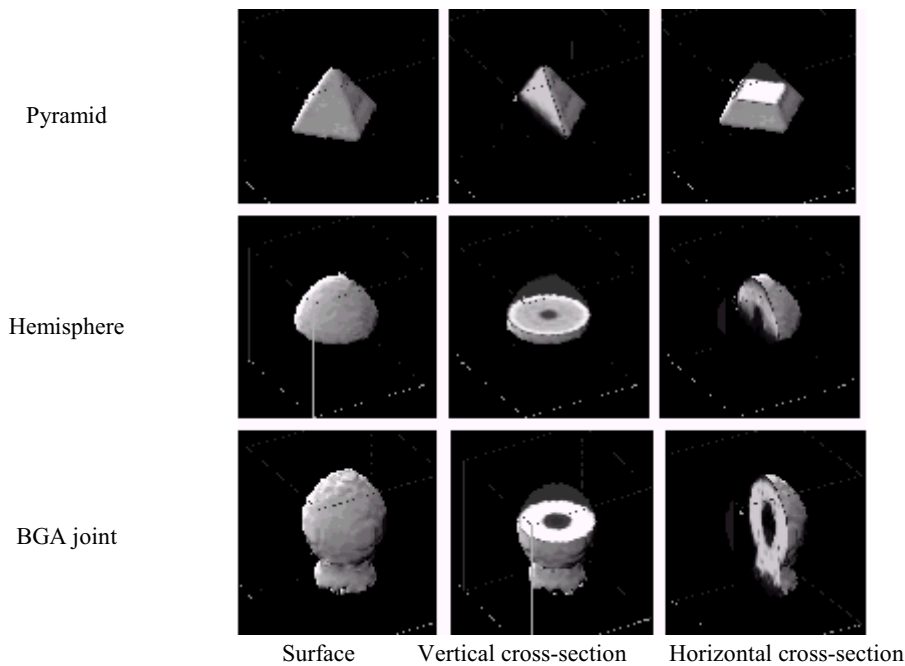


Figure 10. Results of the 3D reconstructions

5. Conclusions

In this paper, USART algorithm for reconstructing the 3D volume of an object was proposed and its advanced performances were compared to that of the conventional one by simulation studies. In this method, the three dimensional volume, the surface and inner structure as well, of an object is reconstructed by a recursive computation method.

In the simulations, 3D reconstruction tasks were conducted on a series of basic objects, a pyramid, a hemisphere and a BGA joint model. The imaging conditions used in the simulations are same as the ones used in the developed x-ray digital tomosynthesis system which can take projected x-ray images from different directions. The objects considered here are within the volume size of $1 \times 1 \times 1 \text{ mm}$ and they are represented by the digitized $40 \times 40 \times 40$ volume elements, voxels.

For the evaluations of the reconstruction process, two different errors were defined. One is the measure of the reconstruction error, which is defined as RMS errors of the reconstructed volume to the reference one. And the other is an image error, which is for the measure of the convergence in the middle of the reconstruct processes.

From the simulation results, USART method was superior to the conventional SART method in that the errors of USART were converged faster and also their final values were smaller than those of the conventional one. The reconstructed volume errors were about 5 ~ 7 % for the objects, which depend on the complexity of the volumes at the same imaging conditions. The calculations for the convergence need about 50 iterations, and after that there was no meaningful change in terms of the image error. It takes approximately 1 second per one update of the whole volume, thus the volume were reconstructed within 1 minute.

The three dimensional imaging technique is useful to the quality inspection or monitoring of tiny electronic parts. Though the resolution of the reconstruction is some low at now for the limitation of the computation time and computer memories, it could be expanded to precision 3D measurements and inspections with the advance of the computer technology and modifications on the algorithm.

ACKNOWLEDGEMENTS

This research was financially supported by Samsung Electronics Corporation as a Korea government supported project of advanced manufacturing system, and conducted through 1999~2000. This research was also partially supported by PoHang Steel Company.

REFERENCES

1. Y.K. Ryu, H.S. Cho, "New optical measuring system for solder joint inspection", *Optics and Lasers in Engineering*, Vol.26, No.6, pp.487-514, 1997.
2. J.H. Kim, H.S. Cho and S.K. Kim, "Visual measurement of a 3-D plane pose by a cylindrical structured light", '93 *Intelligent Robots and Systems*, Yokohama, Japan, 1993.
3. Adams, "X-ray laminography analysis of ultra fine pitch solder connections on ultra-thin boards", *Integrated Circuit Metrology, Inspection, and Process Control V (SPIE)* Vol.1464. 1991, pp 484-497.
4. M. Rooks, B. Benhabib, and K. C. Smith, "Development of an inspection process for ball-grid-array technology using scanned beam x-ray laminography", *IEEE trans. on Components, Packing, and Manufacturing Technology - Part A*. Vol. 18, No 4, December 1995. pp 851-861
5. S.T. Kang, Y.U. Kim and H.S. Cho, "A digital tomosynthesis method for evaluating the soldering states of ball-grid-array joints", 7th *Annual Research Symposium of Transfer of Emerging NDE Technologies*, 1998
6. Y.J. Roh, K.W. Ko, H.S. Cho, H.C. Kim, H.N. Joo, "Inspection of BGA(Ball Grid Array) Solder Joints using X-ray Cross-sectional Images", *Intelligent Systems and Advanced Manufacturing(SPIE)*, Vol. 3836, pp. 168-178, 1999.
7. K.W. Ko, Y.J. Roh, H.S. Cho, Development of an PCB solder joints inspection system using x-ray, research report, Samsung electronics, 1997.
8. Rangarj Rangayyan, Atam Prakash Dhawan, "Algorihtms for limited view computed tomography : an annotated bibliography and a challenge", *Applied Optics*, Vol. 24, No. 23, pp.4000-4012, 1999.
9. Y.J. Roh, H.S. Cho, H.C. Kim, S.K. Kim, "Analysis of X-ray Image Qualities -Accuracy of Shape and Clearness of Image - Using X-ray Digital Tomosynthesis", *Journal of the ICASE*, Vol. 5, No. 5, 558-567, 1999.
10. S.T. Kang and H.S. Cho, "The Quality Evaluation and Improvement for Digital Tomosynthesis Images", *Materials Evaluation*, Vol. 57. No. 8, 841-845, 1999.
11. G.T. Herman, "Algebraic reconstruction techniques can be made computationally efficient", *IEEE tran. On medical imaging*, vol. 12, no.3, sept., pp.600-609, 1993.
12. Y. Censor, "Finite Series-Expansion Reconstruc-tion Methods", *Proceedings of the IEEE*, Vol. 71, No. 3, March, pp.409-418, 1983.
13. Y. Censor, "Row-Action methods for huge and sparse systems and their applications", *SIAM Review*, vol. 23, No. 4, Oct. pp. 444-466, 1981
14. A.H. Andersen and A.C. Kak, " Simultaneous algebraic reconstruction technique(SART) : A superior implementation of the ART algorithm", *Ultrasonic Imaging*, vol 6, pp. 81-94, 1984.
15. J.T. Marti, Zurich, "On the convergence of the discrete ART algorithm for the reconstruction of digital pictures from their projections", *Computing*, vol 21, pp.105-111, 1979.
16. Y.J. Roh, H.S. Cho, "Three Dimensional Shape Reconstruction of BGA Joint using X-ray Images Projected from Different Views", *Korea Automatic Control Conference*, Vol. D, 446-449, 1999.
17. Y.J. Roh, Kuk Won Ko, H.S. Cho, H.C. Kim, H.N. Joo, "The calibration of x-ray digital tomosynthesis system including the compensation of the image distortion", *Intelligent Systems and Advanced Manufacturing(SPIE)*, vol. 3528, 248-259, 1998.
18. S.T.Kang, Arbitrary cross-sectional recognition of 3 dimensional objects using a digital tomosynthesis, Ph.D. thesis, Korea Advanced Institute of Science and Technology, 1998.
19. S. T. Kang, H. S. Cho, "A projection method for reconstructing x-ray images of arbitrary cross-section", *NDT & E International*, vol.32. pp. 9-20, 1999.
20. S.T. Kang, J.H. Jeong, H.G. Song and H.S. Cho, "A new X-Ray cross-sectional imaging system for arbitrary angle inspection of BGA package", *Proc. of NEPCON EAST '97*, pp.109-120, 1997.